

## Guiding and switching by quasi -2D dark spatial solitons

D. Neshev\*, A. Dreischuh\*, S. Dinev\*, L. Windholz

Technical University Graz, Institute of Experimental Physics  
Petersgasse 16, A-8010 Graz, Austria

\* permanent address: Sofia University, Department of Quantum Electronics  
5, J. Bourchier Blvd., BG-1164 Sofia, Bulgaria

### ABSTRACT

Variable number of quasi-2D dark spatial solitons of adjustable transverse velocities could be generated by a proper choice of the initial phase profile (odd/even) and width of crossed dark stripes and the background-beam intensity. The possibility to branch single input probe beam into ordered structures of subbeams is demonstrated numerically in bulk self/induced-defocusing Kerr nonlinear media.

**Keywords:** nonlinear optics, dark optical solitons, beam guiding, beam branching

### 1. INTRODUCTION

The dark spatial optical solitons form a specific class of self-supported beams for which the diffraction is compensated by the beam's self-action in media of negative nonlinearities [1,2]. Because of the negative nonlinear refractive index correction the refractive index itself appears lower in the Dark Spatial Soliton (DSS) wings as compared to this in the vicinity of the intensity-dip. As a consequence, the DSSs should obey guiding properties [3,4]. The same should hold also for a quasi-2D DSS formed by two crossed fundamental 1D Odd Dark Spatial Solitons (ODSSs) [5].

Characteristic for the 1D black ODSS is the abrupt  $\pi$ -phase shift at the zero-intensity position [2,6]. If the phase-jump is absent in the initial phase-portrait of the dark formation (i.e. even formation), the latter splits thresholdless into complementary pairs of diverging gray 1D ODSSs [1]. The increase in the background-beam intensity also causes splitting of the 1D ODSS into an on-axis fundamental 1D ODSS and a diverging pair of gray ODSSs [6]. The splitting of crossed dark formations could be controlled by switching between odd and even dark formations at the entrance face of the Nonlinear Medium (NLM) [7] and by varying the background-beam intensity and/or the initial radii of the odd/even dark formations. The quasi-2D ODSSs generated on this way could cause branching of single input probe beam into discrete variable number of channels (subbeams) and, eventually, with controllable intensity-branching ratios.

### 2. NUMERICAL PROCEDURE AND INITIAL CONDITIONS

Under the slowly-varying envelope approximation the longitudinal evolution of the dark formations in self-defocusing nonlinear media is described by the (2+1)D Nonlinear Schrödinger Equation (NLSE) [8]

$$i \frac{\partial E_D}{\partial z} + \frac{1}{2L_{Diff}^D} \left( \frac{\partial^2}{\partial x^2} + \frac{\partial^2}{\partial y^2} \right) E_D + \frac{1}{L_{NL}^D} |E_D|^2 E_D = 0 \quad (1)$$

where  $L_{Diff}^D = k_D a_D^2$  and  $L_{NL}^D = 1/(k_D n_{2D}^{SPM} |E_D|^2)$  are the Rayleigh diffraction and the nonlinear lengths, respectively,  $k_D$  is the wave-number for the dark wave,  $n_{2D}^{SPM} < 0$  is the nonlinear refractive-index coefficient for Self-Phase Modulation (SPM), and  $E_D$  is the normalized background-beam electric-field amplitude. Since either negligible or moderate probe-beam self-action are considered to accompany the Induced-Phase Modulation (IPM) originating from the dark beam, the probe wave evolution is studied by solving the generalized NLSE

$$i \frac{\partial E_S}{\partial z} + \frac{1}{2L_{Diff}^S} \left( \frac{\partial^2}{\partial x^2} + \frac{\partial^2}{\partial y^2} \right) E_S + \left( \frac{|E_S|^2}{L_{NL}^S} + \frac{\alpha |E_D|^2}{L_{NL}^D} \right) E_S = 0 \quad (2)$$

In Eq. 2  $L_{Diff}^S$  and  $L_{NL}^S$  are the signal diffraction and nonlinear lengths and  $\alpha$  accounts for the relative strength of the IPM. Further to the above notations, the transverse spatial coordinates  $x$  and  $y$  are normalized to the initial transverse extent of the crossed dark formations, i.e. to  $\min(a_{D_x}(z=0), a_{D_y}(z=0))$ . For simplicity  $|k_D - k_S| \ll k_{D,S}$  is assumed in this analysis.

The numerical procedure used for solving Eqs.1-2 is a 2D generalization of the beam-propagation method at  $\alpha = 2$ . Discretization over 1024x1024 grid points is used for both dark and bright formations analyzed. Finite-extent background beam of a super-Gaussian form-factor

$$B(r) = \exp\left\{-\left(r/40\right)^8\right\}, \quad r = (x^2 + y^2)^{1/2} \quad (3)$$

and radius, 40 times larger than the highest width of the 1D dark beams nested in is used. The odd dark stripe at the entrance face of the NLM was described by

$$E_D^O(x, z=0) = E_{D_0} B(r) \tanh(x) \exp(i\Phi) \quad (4a)$$

with

$$\begin{cases} \Phi(y, z=0) = 0 & \text{at } x \leq 0 \\ \Phi(y, z=0) = \pi & \text{at } x > 0 \end{cases}, \quad (4b)$$

whereas for the even one the description

$$E_D^E(x, y, z=0) = E_{D_0} B(r) \{1 - \text{sech}(x)\} \quad (5)$$

is used. The probe beams were assumed to be initially of sech-shapes and widths equal to these of the 1D odd dark formations.

In order to evaluate the guiding quality after the guiding or branching process is completed we assumed that an imaginary array of 3x3 information channels (waveguides of rectangular cross-sections and typical dimension  $x_0$ , four times the diameter of the bright beam at  $z=0$ ) is coupled to the exit face of the NLM. These channels are spaced at  $x_0/2$  and the incoming probe beam is assumed to be on-axially aligned with channel b2 (Fig. 1).

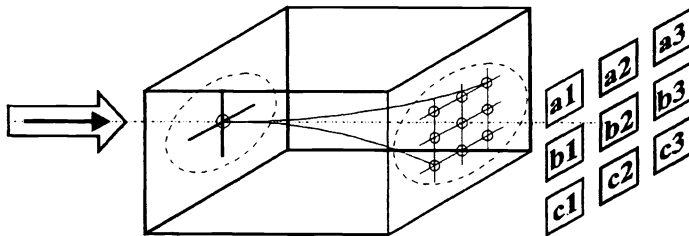


Fig. 1. Disposition scheme and notation of the imaginary information channels coupled to the exit face of the NLM.

### 3. GUIDING OF SIGNAL BEAMS BY QUASI-2D ODSSs

First, the quasi-2D ODSS is modeled as generated initially by two crossed odd dark stripes, i.e.  $E_D = E_D^O(x, z=0)E_D^E(y, z=0)$ . Since each dark stripe is assumed to satisfy exactly the initial conditions required for the formation of an 1D ODSS, no excess of (negative) energy is shaded. Stable propagation of the quasi-2D ODSSs was observed up to  $z = 20L_{Diff}^D$  (Fig. 2a). Only the wings of the 1D ODSSs were influenced by the finite background-beam spreading [8]. The initially hyperbolic-secant-shaped probe beam was found to be guided successfully by the quasi-2D ODSS (Fig.2b). The lack of an axial symmetry in the refractive-index variations induced at negligible probe-wave self-action results in an incomplete guiding of the bright beam along the odd dark stripes and in the formation of a ‘star-like’ transverse energy-density distribution. After a relatively rapid decrease in the probe-beam peak-intensity up to  $z = 1L_{Diff}^D$  it tends to stabilize at an 64%-level of its initial value for  $z > 8L_{Diff}^D$ . The estimation has shown, that only 2.5% of the energy transmitted to channel b2 (integrated over the channel aperture, see Fig.1) becomes redistributed at a negligible cross-talk to channels a1, a3, c1, and c3, and with a cross-talk of 0.22% to channels a2, c2, b1, and b3 at  $z = 20L_{Diff}^D$ . If the initial probe beam intensity is increased up to 50% from this required for an 1D bright soliton under probe-beam self-focusing conditions, the IPM on the dark formation originating from the bright one was found to improve the guiding quality

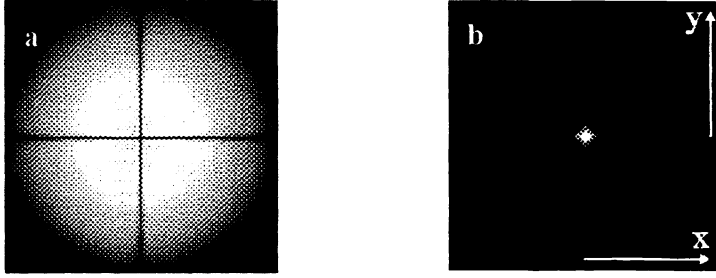


Fig.2. a) Grayscale image of the finite-background super-Gaussian beam with the quasi-2D ODSSs nested in after a propagation path-length of  $z = 20L_{Diff}^D$ ; b) The same for the guided probe wave (twice magnified).

to a practically 100% transmission efficiency to channel b2 (see Fig.1). The star-like structure in the probe beam appeared weaker expressed and the peak-intensity was found to asymptotically tend to 91% of its initial value. No indications for a background modulational instability were found.

#### 4. SIGNAL BEAM BRANCHING INTO TWO AND THREE SUBBEAMS

Such nonlinear evolution can be obtained when crossed 1D odd and even dark soliton stripes are used. Characteristic for this interaction configuration is, that the 1D even dark stripe does split (even at low background intensity) into two diverging gray spatial solitons. Numerically, the initial condition was set to  $E_D(x, y, z=0) = E_D^O(x, z=0)E_D^E(y, z=0)$ , i.e. the two gray ODSSs appear separated in a vertical direction (along the y-axis; see Fig.2a). In Fig.3 we present three slices of

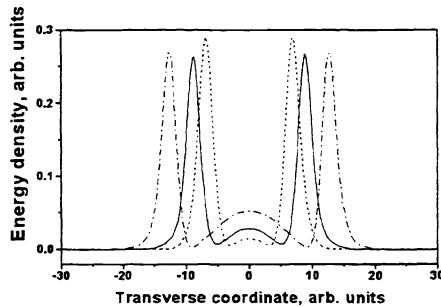


Fig. 3. Cross-section of the branched probe beam along the 1D ODSS stripe at  $a_{D_y}(z=0)/a_{D_x}(z=0) = 0.5$  (long-dashed curve), 1.0 (solid), and 1.5 (short-dashed curve) after nonlinear propagation path-length  $z = 20L_{Diff}^D$ .

the branched probe beam at  $z = 20L_{Diff}^D$  extracted along the fundamental 1D ODSS. The solid curve corresponds to  $a_{D_y}(z=0) = a_{D_x}(z=0)$ , whereas the short- and long-dashed ones - to  $a_{D_y}(z=0)/a_{D_x}(z=0) = 1.5$  and  $0.5$ , respectively. In all the three cases a perfect linearity of the quasi-2D DSS positions vs. nonlinear propagation path-length was found. At no probe-beam self-action the increase in the quasi-2D DSS transverse velocity results in a decrease in the contrast of the quasi-2D branched and guided bright subbeam with respect to the on-axially 1D guided portion of the probe wave (Fig.3). The estimated values for the energy guided to the information channels a2 (and c2) exceeds 11.5, 6.9, and 1.5 times the energy directed to the b2-channel at  $a_{D_y}(z=0)/a_{D_x}(z=0) = 1, 1.5$ , and  $0.5$ , respectively. The branching process completes at approximately  $2.5L_{Diff}^D$  and the profiles given in Fig.3 represent the numerical result obtained at  $z = 20L_{Diff}^D$ . The increase in the intensity of the on-axis peak (long dashed curve) should be attributed to the relatively high transverse velocity of the quasi-2D DSSs resulting in an incomplete branching and guiding. These results are indicative, that a controllable 1:2 and 1:3 probe-wave branching is feasible by adjusting the width of the incoming 1D even dark stripe only. Particular 1D experimental confirmation of these results could be found in [9]. The oscillations on the background beam developed during the formation of the gray odd soliton pair served as perturbations causing modulational instability and leading to the generation of pairs of Optical Vortex Solitons (OVSSs) of opposite topological charges [4]. This is clearly seen on Fig.4 (at  $z = 20L_{Diff}^D$  and  $a_{D_y}(z=0)/a_{D_x}(z=0) = 0.5$ ) and was observed in all the three cases discussed above. The vortices, however, did not influenced remarkably the splitting and guiding of the probe wave in the quasi-2D nonlinear waveguide.

In the presence of a moderate probe-wave self-action under self-focusing conditions the probe beam branching by crossed 1D even and odd dark stripes is found to be sensitive to the initial even dark stripe width  $a_{D_y}(z=0)$ . Let us assume, that the probe beam intensity is high enough to lead to a formation of an 1D bright spatial soliton (in the nonlinear waveguide induced by the 1D ODSS along the y-axis), for instance at  $a_{D_x}(z=0) = a_{D_x}(z=0)$ . The increase of the even dark stripe width  $a_{D_y}(z=0)$  by a factor of 1.5 is found to lead to a signal-beam splitting into three channels (Fig.5) with a

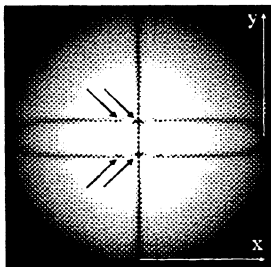


Fig. 4. Grayscale image of the quasi- 2D ODSSs at  $a_{D_y}(z=0)/a_{D_x}(z=0)=0.5$ .

Some of the OVS pairs formed are denoted with arrows.

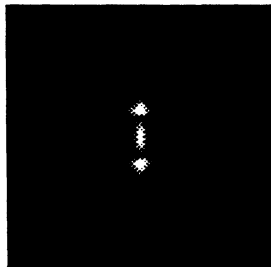


Fig. 5. Branching of a bright probe beam into three subbeams under a non-negligible self-action (see Fig.6 and the text for details).

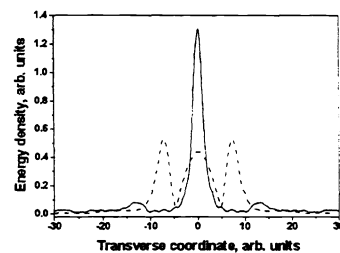


Fig. 6. Branching of the probe wave into three channels with adjustable peak-to-peak energy-density ratio by varying the transverse velocity of the gray solitons at  $a_{D_y}(z=0)/a_{D_x}(z=0)=0.5$  (solid curve) and 1.5 (dashed).

side-lying-to central peak intensity ratio of 1.3 (Fig.6, dashed curve). By decreasing  $a_{D_y}(z=0)$  three times one can significantly increase the transverse velocity  $\lambda_y$  of the gray soliton pair (and of the quasi-2D dark formations), thus decreasing the energy coupling-efficiency to the sidelying channels a2 and c2 to 0.01 of the respective value for the on-axis channel b2 (Fig.6, solid curve). In both cases no substantial energy was coupled to the OVSs generated via the modulational instability of the gray soliton stripes. On this manner a controllable branching of a probe beam into 2 and 3 channels with adjustable peak-to-peak intensity ratio seems feasible.

### 5. SIGNAL BEAM BRANCHING INTO FOUR SUBBEAMS

Let us assume, that two crossed even dark stripes enter the NLM. Each one should evolve in a diverging pair of gray 1D ODSSs. This picture does correspond to an initial electric-field amplitude distribution of the type  $E_D(x,y,z=0) = E_D^E(x,z=0)E_D^E(y,z=0)$ . Fig.7a presents the probe-wave energy-density distribution at  $z = 20L_{Diff}^D$  at  $a_{D_y}(z=0) = a_{D_x}(z=0)$  and  $|E_D^E(z=0)|^2 a_{D_x}^2 = 1$ . As expected, the four quasi-2D dark spatial solitons formed does branch and guide successfully approximately 21.5% of the total probe-beam energy with 12% of the initial probe wave peak energy-density in each channel. One-dimensional cross-sections of the branched beam along the gray stripes is shown in Fig.7b. It was found that a 50% increase in the width of the initial even formations and the associated decrease of their transverse velocity results in 2.5% enhancement in the energy of each branched subbeam at the expense of more pronounced central and side-wing oscillations. In turn, 50% decrease of both  $a_{D_x}(z=0)$  and  $a_{D_y}(z=0)$  results in an incomplete branching of the signal, reduces with approximately 15% the subbeam peak energy-density and each subbeam was estimated to carry 8% of the total incoming probe-wave energy.

### 6. BRANCHING INTO SIX AND SEVEN SUBBEAMS

Up to now we assumed, that the 1D odd dark formation propagates in the form of a fundamental 1D ODSS. At increased background intensity this formation evolves into a fundamental 1D ODSS and a diverging pair of gray ODSSs [6]. Besides this two quasi-2D ODSSs diverging along the 1D ODSS stripe, four additional quasi-2D dark beams does form and diverge radially. These six quasi-2D waveguides appear able to split the incoming probe beam into six distinct subbeams (Fig.8a). The estimated energy branching-efficiencies are 35% for channels a2 and c2, 3.7% for channels a1, a3, c1, and c3, and 6.6% for the on-axis channel b2. The corresponding power-density distributions of the branched probe beam along the x- and the y-axis are presented in Fig.8 with dashed and solid line, respectively. In the generation of Figs.8a,b the quantity  $|E_D^0(z=0)|^2$  was chosen to exceed 1.25 times this required for the fundamental 1D ODSS formation at  $a_{D_x} = 5a_{D_y}$ . It was confirmed numerically, that the spatial position of the four bright subbeams branched in diagonal direction could be controlled by varying the background-beam intensity and/or the initial width of the dark stripes. In view of the above, controllable probe-beam branching into six or seven subbeams seems also feasible being insensitive to the modulational instability and OVS pair formation up to the length of propagation  $z = 20L_{Diff}^D$  reached in our simulations.

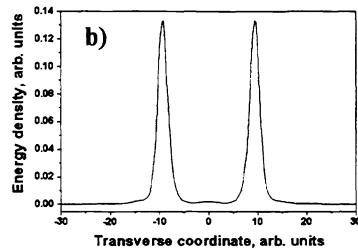
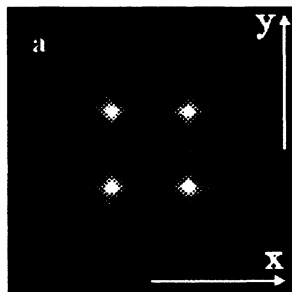


Fig. 7. Grayscale plot (a) and 1D energy-density distribution along the x (y) axis (b) of four subbeams split and guided by pairs of gray ODSSs (see the text for details)

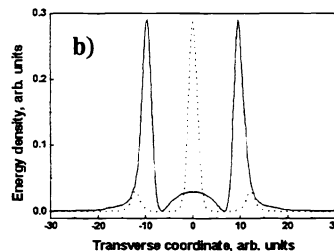
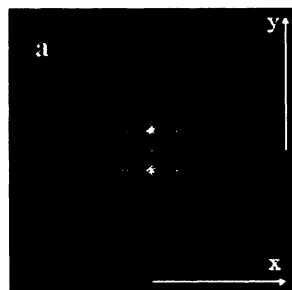


Fig. 8. a) Probe-beam branching into six subbeams

b) One-dimensional energy-density probe-field distribution along the x- (dashed) and y-axis (solid curve) extracted from (a).

$$(z = 20L_{Diff}^D, |E_D^0(z=0)|^2 a_{D_x}^2 = 31.25);$$

## 7. SIGNAL BEAM BRANCHING INTO NINE SUBBEAMS

The last possibility examined in this work is to use pair of crossed 1D odd dark stripes nested on a high-intensity background beam. Each of these stripes does evolve in a fundamental 1D ODSS and a diverging pairs of gray ones. In the particular case of  $|E_D^0(z=0)|^2 = 1.25$  and  $a_{D_x}(z=0) = a_{D_y}(z=0) = 5$  the narrowing of the incoming dark stripes at the initial stage of the gray soliton pairs formation causes probe-wave splitting and guiding mainly along the fundamental 1D ODSSs. Nevertheless, the probe beam seems to branch into nine subbeams at  $z = 20L_{Diff}^D$  (Fig.9a). The probe-beam energy redirected to each one of the channels a1, a3, c1, and c3 is approximately 2% of this transmitted to the on-axis channel b2. The same quantity for the channels a2, c2, b1, and b3 was estimated to be 18%. One dimensional energy-density distribution along the b1-b2-b3 channels is plotted in Fig.9b. Besides the outer-wing satellites guided by the fundamental 1D ODSS, the branched peaks guided by the quasi-2D ODSSs are of a good contrast.

It was found numerically, that the enhancement in  $|E_D^0(z=0)|^2 a_{D_x}^2$  does influence the branching on a different manner depending on whether the background intensity or the stripe-width is increased predominantly. The relative larger increase in  $|E_D^0(z=0)|^2$  causes more pronounced spreading of the background beam and formation of a larger number of OVS-pairs. Besides of this, the contrast in the branched probe subbeams is better at the expense of a lower energy efficiency in each channel (especially in channels a1, a3, c1, and c3) with respect to the case of a predominant enhancement in the initial odd dark stripe width  $a_{D_{x,y}}^0(z=0)$ . It should be noticed also, that the angular offset between the subbeams is less sensitive to  $a_{D_{x,y}}$  of the odd stripe as compared to the background intensity.

## 8. CONCLUSION

In view of the results presented, the controllable branching and guiding of probe beams by quasi-2D dark spatial solitons in discrete varying number of subbeams appears feasible. The effects discussed are based on Kerr-type solitons, but photorefractive media could open the way for constructing practically applicable reconfigurable branchers. It should appear possible to couple each of the channels (see Fig.1) to a separate optical fibre of suitably chosen length. By fast modulating independently the transmission of each channel from 1 to 0 and vice versa and by a subsequent multiplexation of the pulses into a single optical fibre one can ensure ordering of bright pulses with arbitrary intensities in trains (of binary-coded 'bits'), thus reducing the interaction strength within the consecutive pulses of short duration. This idea may appear fruitful for maintaining binary-coded information for launching in the high bit-rate optical communication systems.

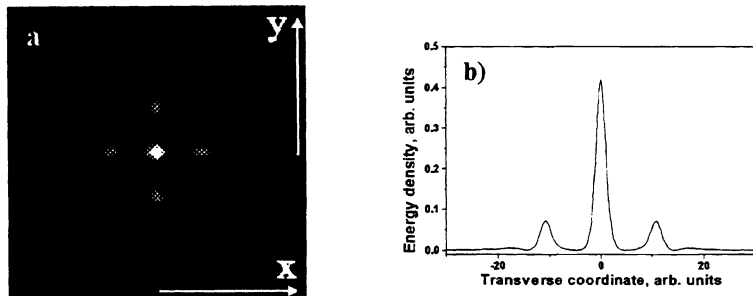


Fig. 9. a) Grayscale image of the probe wave branched by crossed higher-order 1D ODSSs;

b) Probe-wave energy-density distribution along the b1-b2-b3 (e.g. along the a2-b2-c2) channel extracted from (a).

$$(z / L_{Diff}^D = 20 \left| E_D^0(z=0) \right|^2 a_{D_x}^2 = 31.25)$$

## 9. ACKNOWLEDGMENTS

D. N., A. D., and S. D. are grateful to the Technical University Graz, Institute for Experimental Physics, for the warm hospitality and the exciting scientific atmosphere during their research stays supported by the Österreichischer Akademischer Austauschdienst, Austria, and by the CEEPUS Network (A-21). This work was supported by the National Science Foundation, Bulgaria, under contract F-424/1994.

## 10. REFERENCES

1. D. Andersen, D. Hooton, G. Swartzlander, Jr., "Direct measurements of the transverse velocity of dark spatial solitons," *Opt. Lett.* **15**, 783-785 (1990).
2. G. Allan, S. Skinner, D. Andersen, A. Smirl, "Observation of fundamental dark spatial solitons in semiconductors using picosecond pulses," *Opt. Lett.* **16**, 156-158 (1991).
3. R. Jin, M. Liang, G. Khitrova, H. Gibbs, N. Peyghambarian, "Compression of bright optical pulses by dark solitons," *Opt. Lett.* **18**, 494-496 (1993).
4. G. Swartzlander, Jr., C. Law, "Optical vortex solitons observed in Kerr nonlinear media," *Phys. Rev. Lett.* **69**, 2503-2506 (1992).
5. G. Swartzlander, Jr., D. Andersen, J. Regan, H. Yin, A. Kaplan, "Spatial dark soliton stripes and grids in self-defocusing materials," *Phys. Rev. Lett.* **66**, 1583-1586 (1991).
6. W. Tomlinson, R. Hawkins, A. Weiner, J. Heritage, R. Thurston, "Dark optical solitons with finite background pulses," *J. Opt. Soc. Am.* **B6**, 329-334 (1989).
7. A. Marrakchi, S. Habiby, J. Wullert II, "Generation of programmable coherent source arrays using spatial light modulators," *Opt. Lett.* **16**, 931-933 (1991).
8. Yu. Kivshar, X. Yang, "Dark solitons on backgrounds of finite extent," *Opt. Commun.* **107**, 93-98 (1994).
9. B. Luther-Davies, Y. Xiaoping, "Waveguides and Y junctions formed in bulk media by using dark spatial solitons," *Opt. Lett.* **17**, 496-498 (1992).